Nanogel catalysts for the hydrolysis of underivatized disaccharides identified by a fast screening assay

Babloo Sharma and Susanne Striegler[a,]

Department of Chemistry and Biochemistry, 345 North Campus Walk, University of Arkansas, Fayetteville, Arkansas, 72701, USA.

Keywords: Nanogels, glycoside, carbohydrate, hydrolysis, catalysis, screening assay.

ABSTRACT: Applying high throughput synthetic and screening methods for the development of catalytic micro- and nanogels remains challenging due to the nature of the workflow. Typical procedures require the preparation of stable miniemulsions followed by radical polymerization, purification of the obtained gels by extensive extractions or dialysis, and subsequent characterization of physical properties and examination of desired functions. In order to streamline the process, we altered the gel synthesis procedure and developed a screening protocol to identify gel compositions with the desired catalytic function. The assays identify 5 out of 50 synthesized gels from eight different crosslinkers with high potential to hydrolyze carbohydrates. A catalytic proficiency ($k_{cat}/K_M \times k_{non}$) of up to 1.4 x 10^6 and gel activity of 0.8 µmol h^{-1} mg^{-1} was observed placing the synthesized gels among the most proficient catalysts known for the hydrolysis of non-activated glycosidic bonds.

Introduction.

High throughput screening applying Lipinsky's 'rules of five'[1] in structure-activity relationship studies combined with computational analyses[2] and robotics[3] is a frequently used methodology to identify the most promising compounds[4] during drug discovery of low molecular weight targets in a fairly short period of time. The method also allows identification of specific positions in the low molecular weight targets for modifications to achieve desired properties, such as water-[5-7] or fat-solubility[8-11], altered binding affinity by modified strength of H-bonds,[12-14] and others.

When approaching structure-activity relationship studies with functional materials in a similar fashion, the large amount of time to develop and characterize the desired properties in the desired material constitutes one of the biggest challenges.[15] The reasons for the high time demands are generally found in the complexity of the material where large numbers of multifaceted parameters contribute to the overall properties.[15] Nevertheless, successful implementation of high throughput synthesis and screening are nowadays commonly used in a variety of materials including the development of metal organic frameworks (MOFs),[16-18] covalent organic frameworks (COFs),[19] and heterogeneous[20] and homogeneous[21] catalysts.

However, adapting high throughput synthetic and screening methods for the development of catalytic microgels remains challenging.[22-31] Most of the approaches in the field focus on successive synthesis and characterization of the gels in a time- and labor-intensive manner.[22, 24-26, 32-34] This work flow is caused by the need to first form emulsions or miniemulsions of oil in water by ultrasonication, followed by thermal or light-initiated radical polymerization, purification of the obtained gels by extensive extraction or dialysis, and finally the characterization of physical properties and testing for desired functions.

Our previously developed 10 mL scale synthesis for polyacrylate gels coupled with subsequent purification by dialysis is based on the same strategy.[35-36] The approach provides catalysts with the ability to selectively hydrolyze glycosidic bonds in alkaline solution and near neutral pH values.[35-37] Along these lines, a myriad of interactions was probed for their contributions to the formation and stabilization of the transition states of the glycolysis including H-bonding interactions with the immobilized metal complex and the surrounding matrix.[35-39] Very recently, polyacrylate gels were also developed as catalysts for the hydrolysis of underivatized di- and oligosaccharides.[38] However, their analysis added an additional step to the characterization and evaluation of the targeted hydrolysis function, as underivatized saccharides do not possess a chromophore and, therefore, do not facilitate a spectroscopic evaluation of the reaction. Instead, aliquots have to be taken in regular time intervals and subjected to off-line monitoring of the reaction proceedings, i.e. by using chromatographic separation via HPLC coupled with evaporative light scattering detection and comparison to calibration curves for quantitation.[38]

Therefore, streamlining of this complex and time-consuming workflow at any step in the process will provide great advances and savings in the required time and man-power costs. As a first step toward this goal, we developed a new protocol based on multi-well plate assays in place of separate vial syntheses; elaborated a screening assay to correlate gel sizes and catalytic performances during hydrolysis of model glycosides; and lastly linked the results of the screening assays to the ability of the catalysts to hydrolyze a non-derivatized disaccharide. This strategy identifies for each gels series the optimized crosslinking content; discloses the highest observable catalytic turnover; and allows a comparison of the gels during the catalyzed hydrolysis of glycosidic bonds in model substrates and non-activated disaccharides. The details and observations during the development of this approach are summarized and discussed in detail below.

Results and discussion.

Protocol development and catalyst synthesis

As a first step in the outlined approach, eight crosslinkers **1a-h** are selected for the synthesis of polyacrylate gels with a variety of matrix rigidities, chain lengths between branching points, chain polarities, and number of branching points. (**Chart 1**). In a typical synthesis (**Scheme 1**), the wells of a 12-well plate are filled with aliquots of pre-made aqueous stock solutions (aqueous layer) and mixtures of polymerizable monomers and crosslinkers (oil layer). In more detail, the aqueous layer is comprised of 2000 µL of 52 mM TWEEN/SPAN 80/80 solution at a hypophilic-lipophilic balance (HLB) of 14 in mixtures with 5 mM aqueous CAPS buffer solution at pH 10.50 at 0°C; 50 µL of 350 mM aqueous mannose stock solution; and 20 µL of 175 mM aqueous Cu(II) acetate solution. The oil layer is comprised of 0.35 mmol of mixtures of the selected crosslinkers **1a-e** (5 to 100 mol%), corresponding amounts of butyl acrylate (**2**) (95 to 0 mol%), 0.875 mmol of polymerizable pentadentate ligand VBbpdpo (**3**) in DMSO as a solution with 4.2 wt% of ligand, 2 µL of hexadecane, and 40 µL of a 950 mM solution of 2,2'-dimethoxy-2-phenylacetophenone initiator in methanol. The polymerizable complex Cu_2L (L = VBbpdpo (**3**)) forms in situ under the given conditions.[40]

The plate is cooled in an ice-water bath during ultra-sheering of the individual mixtures (30 s each, 40 % amplitude, pulse mode: 5s on, 2s off). Subsequent polymerization is obtained after placing the plate under UV light. To keep the aliquots of the compounds added in the oil layer measurable with common pipets, to maintain a reproducible filling of the wells, and to avoid splashing during sonication, 12-well plates are preferred for this protocol over plates with a larger well number and smaller volumes. All mixtures are prepared in duplicates or triplicates and exposed to UV light for 30-60 min while cooling in water-ice mixtures. Suitable sonication and polymerization times were initially determined in a series of experiments by polymerizing EGDMA (**Tables S1-S5, Figures S1-S5**)

Nano- and microgel screening for size and catalytic turnover with model substrate

Previous results suggest that polyacrylate gels with a minimal size are the catalytically most active gels when compared in their respective polymer series.[35] This observation implies that a fast screening protocol can be developed when combining particle size determinations with catalytic screening. This strategy is subsequently examined by determination of the gel with minimal particle size in each given crosslinker series, and by identification of the catalytically most active polymer in independent experiments. The strategy promises to identify the most active catalytic gels in a series of polymers in a timely manner while avoiding lengthy catalyst purifications based on dialyses or extractions of each gel. Thus, the mean diameters of the particles and their distributions in the synthesized gel suspensions are determined for each polyacrylate series using dynamic light scattering (DLS). The analysis reveals broad particle size distributions with dispersity indices between 0.4 and 0.9 nm in all polymer series at low crosslinking contents. By contrast, monomodal distributions with dispersity indices below 0.4 are observed when higher amounts of the crosslinkers are used during particle synthesis (**Table S6, Figure S6**). In more detail, monomodal distributions of the particles are obtained when the gels are synthesized from at least 60 mol% EGDMA, HDMA or DDMA, 40 mol% DEGDMA, or 25 mol% TEGDMA. Likewise, monomodal distributions are obtained when at least 30 mol% of TMPTA, 20 mol% of PETA or 10 mol% of DPHA are used during material synthesis. The observations indicate that monomodal particle distributions are supported at reduced mobility of the chains forming the particle. Relative to

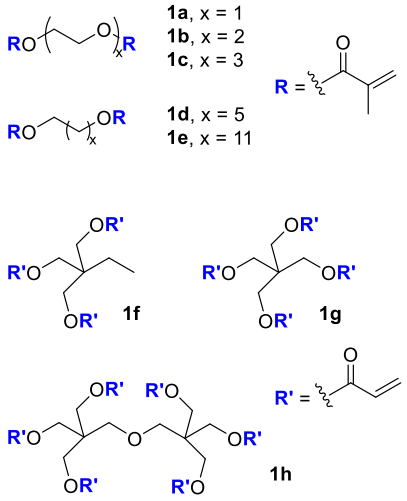

Chart 1. Structures of selected crosslinkers 1

Scheme 1. Synthesis of micro- and nanogels from miniemulsions in 12-well plate assays

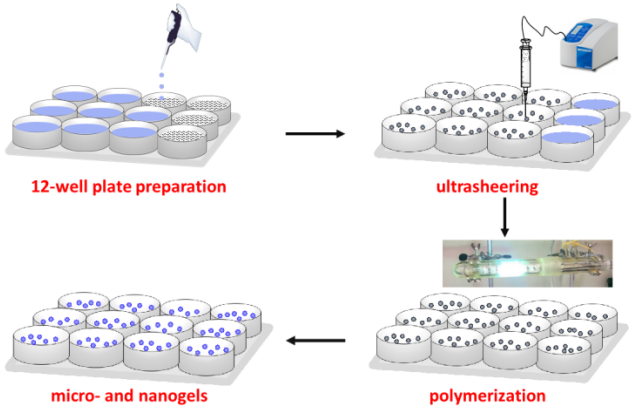

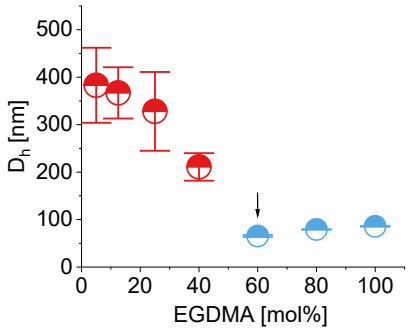

Figure 1. Mean of the particle diameter with the largest peak area in polydisperse gels (red half circle) and intensity-weighted mean of monomodal dispersions (blue half circle) over the respective composition of the gels synthesized from EGDMA (1a)

EGDMA as a standard, this effect can be achieved by increasing the H-bond formation through polar repeating units (DEGDMA,

TEGDMA) and by increasing the number of branching points (TMPTA, PETA, DPHA) in the crosslinker itself.

To visualize the minimal particle size in each gel series, the intensity-weighted mean of the hydrodynamic diameters is plotted over the respective crosslinking content for gels with moderate and narrow distributions (**Figures 1 and S7**). For gels with broad distributions, the mean of the peak with the largest area is plotted likewise in the same graph. The gel with the lowest diameter marked with an arrow. The results indicate the formation of monomodal nanogels with minimal hydrodynamic diameters D_h for crosslinkers **1a-1c, 1g-1h,** while microgels are obtained from crosslinkers **1d-1e** (**Table 1**). In contrast to all other gels, the dynamic light scattering experiments for TMPTA-containing gels do not indicate monomodal size distributions over the evaluated crosslinker range (**Figure S6f, Table S6f, Figure S7F**). A repetition of the material synthesis did not alter the results. As macromolecular catalysts with broad dispersity are undesirable, TMPTA-derived gels are not considered further in this study.

In a second set of characterization experiments, aliquots of the unpurified gels are used to catalyze the hydrolysis of 4-methylumbelliferyl *N*-acetyl-*β*-D-glucosaminide (**4**) in 50 mM aqueous HEPES buffer (**Scheme 2**). The developed assay uses 96-well plates and constant concentrations of substrate (2 mM) and catalyst (8 μM) in each well at an overall nominal volume of 200 μL. The formation of 4-methylumbelliferone (**5**) is followed at 37 °C by recording changes in arbitrary fluorescence units by reads at 465 nm (λ_{ex} = 360 nm) over 6 h in 10 min intervals. While kinetic parameters cannot be deduced from such an assay, changes in the amount of product formation over time can be gathered and correlated to the crosslinking content of each gel (**Figures 2-3 and S8, Table S7**).

A comparison between the maximized slopes for the hydrolyses of **4** and the sizes of the gels used as catalysts for the glycoside hydrolysis (**Figure 2**) shows a correlation between the steepest slopes of the initial rates of the reaction and the sizes of the respective nano- and microgels. In short, the smallest particles are the most efficient catalysts in each polymer series. A comparison *across* the polyacrylate series reveals that the nanogels derived from crosslinkers **1a-c** are more efficient in the hydrolysis of the glycosidic bond in **4** than microgels derived from crosslinkers **1d-e** and **1g-h** (**Figure 2**).

Prior to catalytic hydrolysis of a reducing disaccharide, five selected nanogels with EGDMA (60 mol%), DEGDMA (40 mol%), TEGDMA (25 mol%), PETA (20 mol%) and DPEHA (10 mol%) crosslinkers are re-synthesized in 10 mL scale,[35] purified by dialysis following previously described procedures,[35-36] and characterized for their ligand content. The ligand concentration is derived as a percentage of its theoretical value using gravimetric analyses during gel syntheses as the non-dialyzable TWEEN-SPAN surfactant system does not allow isolation of the gels (**Figure S9, Table S8**). At the 60 min mark, the polymerization has progressed to 94% for EGDMA, 90% for DEGDMA, 91% for TEGDMA, 90 % for PETA, and 91 % for DPEHA accounting for an overall catalyst concentration in the gels between 105 and 142 μM. The amount of immobilized VBbpdpo ligand also serves as a measure for the concentration of the binuclear Cu(II) complex derived from the immobilized ligand. Isothermal titration calorimetry based on previously developed assays showed quantitative reloading of Cu(II) ion relative to the identified ligand concentrations for all gels (**Figure S10**). As the TWEEN-SPAN surfactant system is non-dialyzable, the thermal stability of the herein described polyacrylate nanogels is not determined. However, related polyacrylate microgels obtained in a SDS surfactant system were previously evaluated and may give an estimate of the stability of the materials under investigation here (see Supporting Information).[41]

The five selected gels are then used as catalysts to hydrolyze non-derivatized carbohydrates.[35]

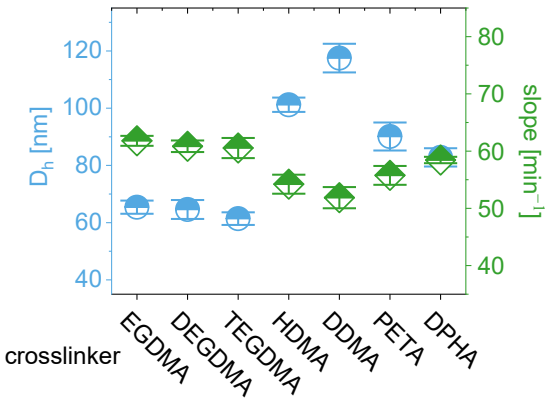

Figure 2. Correlation between steepest slope and lowest hydrodynamic diameter in selected gels

Table 1. Minimal hydrodynamic diameters D_h of selected monomodal gels from crosslinkers 1a-h

Entry	Crosslinker	mol%	D_h [nm]
1	EGDMA (**1a**)	60	65 ± 2
2	DEGDMA (**1b**)	40	65 ± 3
3	TEGDMA (**1c**)	25	62 ± 2
4	HDMA (**1d**)	60	101 ± 3
5	DDMA (**1e**)	60	118 ± 10
6	TMPTA (**1f**)	30	--
7	PETA (**1g**)	20	90 ± 5
8	DPEHA (**1h**)	10	83 ± 3

Scheme 2. Hydrolysis of model substrate 4

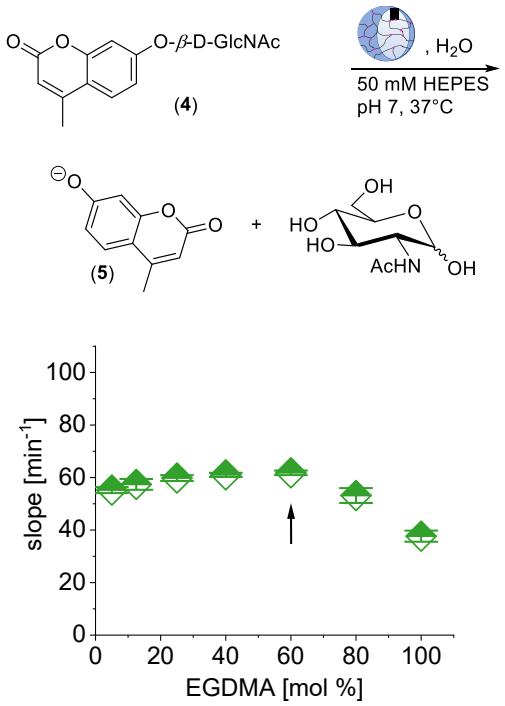

Figure 3. Change of arbitrary fluorescent units per time for the hydrolysis of model substrate 4 in correlation to the content of crosslinker 1a in corresponding gels.

To assess the quality of the developed pre-screening assays for the identification of optimized catalysts, the catalytic hydrolysis of turanose (**6**) into glucose (**7**) and fructose (**8**) is examined. The disaccharide consists of a non-reducing glucopyranosyl unit with a 1→3 α-linkage to a reducing fructose moiety (**Scheme 3**). While the reducing fructose unit in **6** may exist in equilibria of pyranosyl, furanosyl and open chain structures, the *β*-fructopyranosyl form (65%) is dominant in aqueous solution and shown here.[42] Typically, non-activated disaccharides (such as **6**) are more difficult to hydrolyze than model substrates (such as **4**) with good leaving groups.

Nanogels for catalytic disaccharide hydrolysis

In the following kinetic assay, 250 µL aliquots of 21-28 µM purified polyacrylate gels are preheated at 60 °C in 2000 µL of aqueous sodium hydroxide solution and treated with 250 µL turanose solution in six concentrations between 25 and 500 mM. The resulting concentrations of substrate (2.5-50 mM) and catalyst (2-3 µM) ensure steady-state conditions in the assay and allow analysis of the obtained data by Michael is-Menten methods. Along these lines, six aliquots (100 µL) of the reaction mixture are taken in regular time intervals over 3 h, neutralized with 12 mM hydrochloric acid, flash frozen, and stored at -20 °C until analysis by HPLC. The formation of glucose (**7**, R_f = 8.2 min) and the consumption of turanose (**6**, R_f = 11.5 min) is followed by analysis of their respective peak area. A Luna amino column is used as the stationary phase and isocratic 80% acetonitrile as the mobile phase. The sugar amounts are quantified by comparison to calibration curves.

Plots of the resulting initial rates corrected for the catalyst concentration over the substrate concentration yield kinetic rate constants (k_{cat}) and substrate affinities (K_M) using the Michaelis-Menten equation (**Table 2**). All experiments are performed in duplicates or triplicates, and the data are given as averages thereof. Catalyst-free control reactions of the substrate hydrolysis are done under comparable conditions yielding the rate constant for the uncatalyzed reaction (k_{non}). For the discussion of the performance of the polyacrylate gels, their catalytic efficiency (k_{cat}/K_M) and proficiency ($k_{cat}/(K_M \times k_{non})$) disclose the contributions of the different matrix compositions at the given crosslinker amounts.

The proficiency of the optimized catalysts to hydrolyze turanose is up to 1.4×10^6 and thus comparable to proficiency of other catalysts for the hydrolysis of a model substrate with an activated glycosidic bond.[43] This result is notable as the hydrolyzed disaccharide used here is underivatized and the leaving group is non-activated. Within experimental error, the turanose hydrolysis is comparably catalyzed by nanogels synthesized from **1a-c** at their identified crosslinking content, while gels **1e-f** are somewhat less efficient **(Figure 4)**. This observation indicates a better stabilization of the transition state of the reaction by crosslinkers promoting hydrogen bondings (**1a-c**) than by crosslinkers promoting a higher crosslinking density through increased number of branching points (**1e-f**). Overall, the results mirror the results of the above-described screening assays and emphasize that the combination of screening assays for catalytic activity and size allows the identification of catalytically proficient gels circumventing tedious efforts in synthesis and purification of a large number of gels.

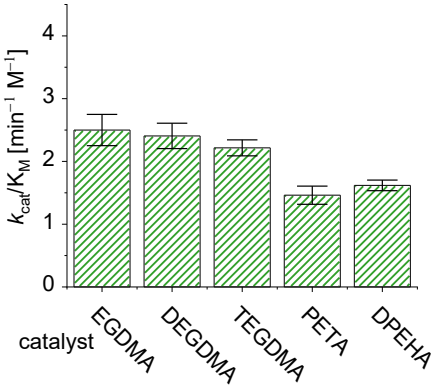

Figure 4. Efficiency (k_{cat}/K_M) of selected polyacrylate nanogels for the hydrolysis of turanose (6)

Scheme 3. Gel-catalyzed hydrolysis of turanose (6)

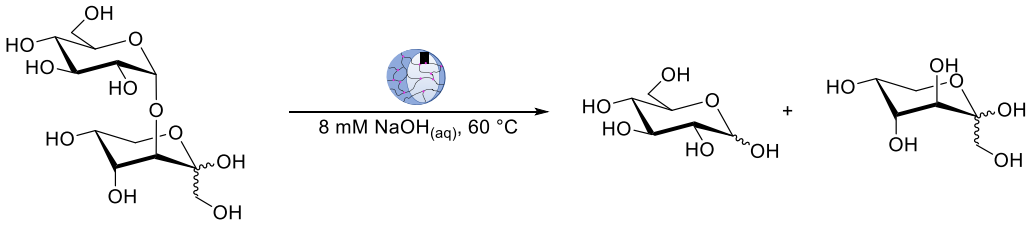

Table 2. Kinetic parameters for the gel-catalyzed hydrolysis of turanose (6)

Crosslinker, **1**	$k_{cat} \pm \Delta k_{cat} \times 10^{-3}$[min^{-1}]	$K_M \pm \Delta K_M$ [mM]	k_{cat}/K_M [min^{-1}M^{-1}]	$k_{cat}/(K_M \times k_{non})$
EGDMA, **1a**	19.2 ± 1.35	7.66 ± 2.50	2.5	1,400,000
DEGDMA, **1b**	20.0± 1.20	8.39 ± 1.22	2.4	1,400,000
TEGDMA, **1c**	20.6 ± 0.84	9.29 ± 0.764	2.2	1,300,000
PETA, **1e**	30.9 ± 2.2	21.2 ± 2.50	1.5	820,000

DPEHA, **1f**	38.3 ± 1.41	23.7 ± 1.87	1.6	910,000

k_{non} = 1.78 ± 0.07 × 10^{-6} $min^{-1}M^{-1}$ in 8 mM aqueous NaOH solution

Conclusions

The elaborated synthesis and screening assays streamline the catalyst development and provide several advantages over previously established synthesis and characterization protocols. In more detail, the revised procedures allow the synthesis of 12 instead of 4 polymers per hour, and enable catalytic screening using a model substrate in a 96-well plate assay before in-depth purification and characterization of a large number of gels. In the current study, the revised protocol narrows down the evaluation and characterization of 51 polyacrylate gels synthesized from 8 crosslinkers to 5 pre-selected gels with known composition and high potential for a maximized performance during the catalytic hydrolysis of glycosidic bonds. A catalytic proficiency of up to 1.4 x 10^6 for the hydrolysis of the non-activated glycosidic bond in turanose at 60 °C is achieved by EGDMA-based nanogels. Similar, yet slightly lower proficiencies are determined for DEGDMA- and TEGDMA-based nanogels possessing longer glycol chains in their respective polymer backbones. This observation is ascribed to increased H-bond interactions and higher binding interactions between substrate, products and gel backbones of **1b** and **1c** that possess one and two more glycol units than **1a** (**Table 2**).

While several types of biomimetic catalysts for the hydrolysis of glycosidic bonds are known, most of these entities demonstrate their activity by hydrolyzing activated glycosidic bonds in model substrates in acidic solutions and elevated temperatures. A notable example includes the evaluation of catalytic antibodies with proficiencies up to 1× 10^9 for the hydrolysis of glycosidic bonds.[44-45]

Reports for the hydrolysis of underivatized carbohydrates and non-activated glycosidic bonds are less frequent.[46-47] In this context, Ce(IV) ions were shown to hydrolyze disaccharides between 40 and 80°C in 40 mM TRIS buffer at pH 7.0 or more acidic conditions more than 25 years ago.[47] While kinetic parameters for the hydrolysis of sucrose are reported (k_{cat} = 2.26 x 10^{-3} min^{-1}; K_M = 3720 mM),[47] a value-by-value comparison of the ion-induced catalytic activity to the herein described gels remains limited due to the largely different reaction conditions, vastly different substrate affinities, pH values of the reactions, and temperatures, and the lack of data for the uncatalyzed reaction under the respective reaction conditions.[48] More recently, a synergistic hydrolysis of cellulose by a blend of cellulose-mimicking polymeric nanoparticle catalysts is reported with activities of up 0.486 ± 0.011 µmol mg^{-1} h^{-1} at 90 °C and 0.512 ± 0.001 µmol mg^{-1} h^{-1} at 100 °C at pH 6.5.[46] When expressing the catalytic performance of the herein developed gels likewise as product amount formed over time in dependence of the catalyst amount, the activities calculate to 0.350 to 0.840 µmol mg^{-1} h^{-1} (**Tables S9-S10**). Thus, the synthesized gels place overall among catalysts with highest proficiency in the hydrolysis of non-activated glycosidic bonds. The elaborated screening and synthesis protocols are likely to open new pathways for further development of biomimetic catalysts in near future.

ASSOCIATED CONTENT

AUTHOR INFORMATION

Corresponding Author

*phone: +1-479-575-5079; fax: +1-479-575-4049 ; Email: Susanne.Striegler@uark.edu.

ORCID

Babloo Sharma: 0000-0002-0265-322X
Susanne Striegler: 0000-0002-2233-3784

Author Contributions

The manuscript was written through contributions of all authors. All authors have given approval to the final version of the manuscript.

Supporting Information. Plots for the screening for the hydrodynamic diameters and catalytic performance of gels derived from crosslinkers **1a-h**; gravimetric analysis plots; a representative graph for the metal ion reloading into a gel synthesized from 25 mol % of TEGDMA (**1c**) using isothermal titration calorimetry. This material is available free of charge via the Internet at http://pubs.acs.org.

ACKNOWLEDGMENT

Funding Sources

Support of this research to S.S. from the National Science Foundation (CHE-1854304) is gratefully acknowledged.

Notes

The authors declare no competing financial interests.

REFERENCES

1. Lipinski, C. A.; Lombardo, F.; Dominy, B. W.; Feeney, P. J., Experimental and computational approaches to estimate solubility and permeability in drug discovery and development settings Adv. Drug Deliv. Rev. 2001, 46 (1), 3-26.
2. Maier, W. F.; Stöwe, K.; Sieg, S., Combinatorial and High-Throughput Materials Science Angew. Chem., Int. Ed. Engl. 2007, 46 (32), 6016-6067.
3. Bogue, R., Robots in the laboratory: a review of applications Ind. Robot 2012, 39, 113-119.
4. Bleicher, K. H.; Böhm, H.-J.; Müller, K.; Alanine, A. I., Hit and lead generation: beyond high-throughput screening Nat. Rev. Drug Discov. 2003, 2 (5), 369-378.
5. Mogal, P. S.; Dode, R. H.; Pansare, J. J.; Pagar, U. N.; Surawase, R. K., Solid dispersion: a magnificent approach to improve solubility of poorly soluble drugs Eur. J. Biomed. Pharm. Sci. 2021, 8, 171-176.
6. Nagare, D. M.; Jate, V. G.; Jadhav, S. N., Review on :"Solubility enhancement techniques for poorly soluble drugs" Int. J. Univers. Pharm. Bio Sci. 2021, 10, 30-44.
7. Gupta, S.; Sawarkar, S.; Ravikumar, P., Solubility enhancement of poorly water soluble protease inhibitor Int. J. Pharm. Sci. Res. 2016, 7, 252-258.
8. Sangaralingham, S. J.; Whig, K.; Peddibhotla, S.; Kirby, R. J.; Sessions, H. E.; Maloney, P. R.; Hershberger, P. M.; Mose-Yates, H.; Hood, B. L.; Vasile, S.; Pan, S.; Zheng, Y.; Malany, S.; Burnett, J. C., Jr., Discovery of small molecule guanylyl cyclase A receptor positive allosteric modulators Proc. Natl. Acad. Sci. U. S. A. 2021, 118, e2109256118.
9. Dato, F. M.; Maassen, A.; Goldfuss, B.; Pietsch, M., Characterization of fatty acid amide hydrolase activity by a fluorescence-based assay Anal. Biochem. 2018, 546, 50-57.
10. Takamiya, M.; Sakurai, M.; Teranishi, F.; Ikeda, T.; Kamiyama, T.; Asai, A., Lead discovery for mammalian elongation of long chain fatty acids family 6 using a combination of high-

throughput fluorescent-based assay and RapidFire mass spectrometry assay Biochem. Biophys. Res. Commun. 2016, 480, 721-726.

11. Mosgaard, M. D.; Sassene, P.; Mu, H.; Rades, T.; Mullertz, A., Development of a high-throughput in vitro intestinal lipolysis model for rapid screening of lipid-based drug delivery systems Eur. J. Pharm. Biopharm. 2015, 94, 493-500.

12. Clyde, A.; Galanie, S.; Kneller, D. W.; Ma, H.; Babuji, Y.; Blaiszik, B.; Brace, A.; Brettin, T.; Chard, K.; Chard, R.; Coates, L.; Foster, I.; Hauner, D.; Kertesz, V.; Kumar, N.; Lee, H.; Li, Z.; Merzky, A.; Schmidt, J. G.; Tan, L.; Titov, M.; Trifan, A.; Turilli, M.; Van Dam, H.; Chennubhotla, S. C.; Jha, S.; Kovalevsky, A.; Ramanathan, A.; Head, M. S.; Stevens, R., High-Throughput Virtual Screening and Validation of a SARS-CoV-2 Main Protease Noncovalent Inhibitor J. Chem. Inf. Model. 2022, 62, 116-128.

13. Peng, C.; Li, Y.-H.; Yu, C.-W.; Cheng, Z.-H.; Liu, J.-R.; Hsu, J.-L.; Hsin, L.-W.; Huang, C.-T.; Juan, H.-F.; Chern, J.-W.; Cheng, Y.-S., Inhibitor development of MTH1 via high-throughput screening with fragment based library and MTH1 substrate binding cavity Bioorg. Chem. 2021, 110, 104813.

14. Iqbal, D.; Rehman, M. T.; Dukhyil, A. B.; Rizvi, S. M. D.; Al Ajmi, M. F.; Alshehri, B. M.; Banawas, S.; Khan, M. S.; Alturaiki, W.; Alsaweed, M., High-throughput screening and molecular dynamics simulation of natural product-like compounds against Alzheimer's disease through multitarget approach Pharmaceuticals 2021, 14, 937.

15. Clayson, I. G.; Hewitt, D.; Hutereau, M.; Pope, T.; Slater, B., High Throughput Methods in the Synthesis, Characterization, and Optimization of Porous Materials Adv. Mater. 2020, 32 (44), 2002780.

16. Stock, N.; Biswas, S., Synthesis of Metal-Organic Frameworks (MOFs): Routes to Various MOF Topologies, Morphologies, and Composites Chem. Rev. 2012, 112 (2), 933-969.

17. Cohen, S. M., Postsynthetic Methods for the Functionalization of Metal–Organic Frameworks Chem. Rev. 2012, 112 (2), 970-1000.

18. Bétard, A.; Fischer, R. A., Metal–Organic Framework Thin Films: From Fundamentals to Applications Chem. Rev. 2012, 112 (2), 1055-1083.

19. Geng, K.; He, T.; Liu, R.; Dalapati, S.; Tan, K. T.; Li, Z.; Tao, S.; Gong, Y.; Jiang, Q.; Jiang, D., Covalent Organic Frameworks: Design, Synthesis, and Functions Chem. Rev. 2020, 120 (16), 8814-8933.

20. McCullough, K.; Williams, T.; Mingle, K.; Jamshidi, P.; Lauterbach, J., High-throughput experimentation meets artificial intelligence: a new pathway to catalyst discovery Phys. Chem. Chem. Phys. 2020, 22 (20), 11174-11196.

21. Renom-Carrasco, M.; Lefort, L., Ligand libraries for high throughput screening of homogeneous catalysts Chem. Soc. Rev. 2018, 47 (13), 5038-5060.

22. Nauman, N.; Boyer, C.; Zetterlund, P. B., Miniemulsion polymerization via membrane emulsification: Exploring system feasibility for different monomers Colloid Polym. Sci. 2022, 300, 309-317.

23. Jin, L.; Tian, J.; Li, J.; Yan, X.; Qi, D., Investigation of the water barrier properties of graft copolymer latex films of acrylate and poly(dimethylsiloxane) macromonomers synthesized by RAFT miniemulsion polymerization Eur. Polym. J. 2022, 168, 111107.

24. Glasing, J.; Cazotti, J. C.; Fritz, A. T.; Szych, L. S.; Fakim, D.; Smeets, N. M. B.; Cunningham, M. F., Starch nanoparticles as Pickering emulsifiers in miniemulsion polymerization of styrene Can. J. Chem. Eng. 2022, 100, 752-766.

25. Dogan-Guner, E. M.; Schork, F. J.; Brownell, S.; Schueneman, G. T.; Shofner, M. L.; Meredith, J. C., Encapsulation of cellulose nanocrystals into acrylic latex particles via miniemulsion polymerization Polymer 2022, 240, 124488.

26. De San Luis, A.; Kleinsteuber, M.; Schuett, T.; Schubert, S.; Schubert, U. S., Miniemulsion polymerization at low temperature: A strategy for one-pot encapsulation of hydrophobic anti-inflammatory drugs into polyester-containing nanoparticles J. Colloid Interface Sci. 2022, 612, 628-638.

27. Guimaraes, T. R.; Delafresnaye, L.; Zhou, D.; Barner-Kowollik, C.; Zetterlund, P. B., Multisegmented polymers via step-growth and RAFT miniemulsion polymerization Polym. Chem. 2021, 12, 5952-5962.

28. Machado, T. O.; Beckers, S. J.; Muller, B.; Landfester, K.; Wurm, F. R.; Sayer, C.; de, A. P. H. H.; Fischer, J., Bio-Based Lignin Nanocarriers Loaded with Fungicides as a Versatile Platform for Drug Delivery in Plants Biomacromolecules 2020, 21, 2755-2763.

29. Costa, C.; Wagner, M.; Musyanovych, A.; Landfester, K.; Sayer, C.; Araujo, P. H. H., Decrease of methyl methacrylate miniemulsion polymerization rate with incorporation of plant oils Eur. J. Lipid Sci. Technol. 2016, 118, 93-103.

30. Barrios, S. B.; Petry, J. F.; Weiss, C. K.; Petzhold, C. L.; Landfester, K., Polymeric coatings based on acrylic resin latexes from miniemulsion polymerization using hydrocarbon resins as osmotic agents J. Appl. Polym. Sci. 2014, 131, 40569/1-40569/9.

31. Landfester, K.; Mailaender, V., Nanocapsules with specific targeting and release properties using miniemulsion polymerization Expert Opin. Drug Delivery 2013, 10, 593-609.

32. Elzayat, A.; Adam-Cervera, I.; Alvarez-Bermudez, O.; Munoz-Espi, R., Nanoemulsions for synthesis of biomedical nanocarriers Colloids Surf. B 2021, 203, 111764.

33. Jenjob, R.; Phakkeeree, T.; Seidi, F.; Theerasilp, M.; Crespy, D., Emulsion Techniques for the Production of Pharmacological Nanoparticles Macromol. Biosci. 2019, 19, e1900063.

34. Jenjob, R.; Seidi, F.; Crespy, D., Recent advances in polymerizations in dispersed media Adv. Colloid Interface Sci 2018, 260, 24-31.

35. Sharma, B.; Striegler, S., Nonionic Surfactant Blends to Control the Size of Microgels and Their Catalytic Performance during Glycoside Hydrolyses ACS Catal. 2020, 10 (16), 9458-9463.

36. Sharma, B.; Pickens, J. B.; Striegler, S.; Barnett, J. D., Biomimetic Glycoside Hydrolysis by a Microgel Templated with a Competitive Glycosidase Inhibitor ACS Catal. 2018, 8 (8), 8788–8795.

37. Sharma, B.; Striegler, S., Tailored Interactions of the Secondary Coordination Sphere Enhance the Hydrolytic Activity of Cross-Linked Microgels ACS Catal. 2019, 9 (3), 1686-1691.

38. Striegler, S.; Sharma, B.; Orizu, I., Microgel-catalyzed hydrolysis of non-activated disaccharides ACS Catal. 2020, 10 (24), 14451-14456.

39. Sharma, B.; Striegler, S.; Whaley, M., Modulating The Catalytic Performance Of An Immobilized Catalyst With Matrix Effects – A Critical Evaluation ACS Catal. 2018, 8 (8), 7710-7718.

40. Striegler, S.; Pickens, J. B., Discrimination of chiral copper(II) complexes upon binding of galactonoamidine ligands Dalton Trans. 2016, 45, 15203-15210.

41. Sharma, B.; Striegler, S., Crosslinked Microgels as Platform for Hydrolytic Catalysts Biomacromolecules 2018, 19 (4), 1164–1174.

42. Collins, P.; Robin, F., Monosaccharides - their chemistry and their roles in natural products. John Wiley & Sons: New York, 1995, p. 41.

43. Sharma, B.; Striegler, S., Polarity and critical micelle concentration of surfactants support the catalytic efficiency of nanogels during glycoside hydrolyses ACS Catal. 2022, 12 (15), 8841–8847.

44. Yu, J.; Choi, S. Y.; Moon, K. D.; Chung, H. H.; Youn, H. J.; Jeong, S.; Park, H.; Schultz, P. G., A glycosidase antibody elicited against a chair-like transition state analog by in vitro immunization Proc. Natl. Acad. Sci. U. S. A.. 1998, 95 (6), 2880-2884.

45. So-Young, C.; Hyun Joo, Y.; Jaehoon, Y., Enzymatic Characterization of Glycosidase Antibodies Raised against a Chair Transition State Analog and the Retained Catalytic Activity from the Expressed Single Chain Antibody Fragments Mol. Cells 2002, 13 (3), 463-469.

46. Zangiabadi, M.; Zhao, Y., Synergistic Hydrolysis of Cellulose by a Blend of Cellulase-Mimicking Polymeric Nanoparticle Catalysts J. Am. Chem. Soc. 2022, 144 (37), 17110-17119.

47. Ishida, H.; Seri, K.-i., Efficient Catalytic Hydrolysis of Disaccharides by Cerium(IV) Ion at pH 7 Chem. Lett. 1997, 26 (4), 379-380.

48. Miller, B. G.; Wolfenden, R., Catalytic Proficiency: The Unusual Case Of Omp Decarboxylase Ann. Rev. Biochem. 2002, 71, 847-885.

Graphical abstract